

Global observations of nitric oxide in the thermosphere

C. A. Barth,¹ K. D. Mankoff,¹ S. M. Bailey,² and S. C. Solomon³

Received 24 April 2002; revised 23 September 2002; accepted 27 September 2002; published 18 January 2003.

[1] Nitric oxide density in the lower thermosphere (97–150 km) has been measured from the polar-orbiting Student Nitric Oxide Explorer (SNOE) satellite as a function of latitude, longitude, and altitude for the 2 1/2 year period from 11 March 1998 until 30 September 2000. The observations show that the maximum density occurs near 106–110 km and that the density is highly variable. The nitric oxide density at low latitudes correlates well with the solar soft X-ray irradiance (2–7 nm), indicating that it is the solar X-rays that produce thermospheric nitric oxide at low and midlatitudes. Nitric oxide is produced at auroral latitudes (60°–70° geomagnetic) by the precipitation of electrons (1–10 keV) into the thermosphere. During high geomagnetic activity, increased nitric oxide may be present at midlatitudes as the result of meridional winds that carry the nitric oxide equatorward.

INDEX TERMS: 0355 Atmospheric Composition and Structure: Thermosphere—composition and chemistry; 0358 Atmospheric Composition and Structure: Thermosphere—energy deposition; 0310 Atmospheric Composition and Structure: Airglow and aurora; 2704 Magnetospheric Physics: Auroral phenomena (2407); *KEYWORDS:* nitric oxide, solar soft x-rays, lower thermosphere, auroral electrons, SNOE

Citation: Barth, C. A., K. D. Mankoff, S. M. Bailey, and S. C. Solomon, Global observations of nitric oxide in the thermosphere, *J. Geophys. Res.*, 108(A1), 1027, doi:10.1029/2002JA009458, 2003.

1. Introduction

[2] Global observations of nitric oxide in the thermosphere have been made from the Student Nitric Oxide Explorer (SNOE), a low-altitude, polar-orbiting satellite. Nitric oxide is an important constituent of the thermosphere because of its chemical reactivity, its ionospheric activity, and its radiative properties. The density distribution of nitric oxide may also be used as an indicator of the temporal and spatial distribution of energy deposition into the thermosphere.

[3] The first observations of thermospheric nitric oxide from an Earth-orbiting satellite were made in 1968 from the Orbiting Geophysical Observatory (OGO-4) with a nadir-viewing ultraviolet spectrometer measuring the fluorescent scattering of ultraviolet solar radiation by nitric oxide. Limited mapping of the latitudinal variation in nitric oxide density led to the realization that there was more nitric oxide at high latitudes than at low latitudes [Rusch and Barth, 1975]. The first limb-scanning measurements of nitric oxide with the fluorescent scattering technique were made from the Atmosphere Explorer satellites [Barth *et al.*, 1973]. The 57° inclination of the orbit of AE-C limited global coverage to low and midlatitudes. The operational lifetime of the polar-orbiting AE-D was too short to achieve extensive coverage. The first limb-scanning observations of nitric

oxide from a satellite with a Sun-synchronous orbit were conducted with the ultraviolet spectrometer on the Solar Mesosphere Explorer (SME). Measurements of nitric oxide at both equatorial and auroral latitudes were made over a four and a half year period [Barth, 1992]. However, since observations were made only on one or two orbits per day, global measurements of the daily distribution of nitric oxide were not obtained. The observations reported in this paper are the first global measurements of nitric oxide in the thermosphere using the limb-scanning technique. They cover the two and a half year period from 11 March 1998 to 30 September 2000.

[4] Two mechanisms have been identified as sources of nitric oxide in the thermosphere. At high latitudes, the precipitation of auroral electrons (1–10 keV) produces ionization that leads to the production of nitric oxide [Gerard and Barth, 1977]. At low latitudes, the predominant source is now thought to be solar soft X-rays. From an analysis of the time variation of equatorial nitric oxide, the hypothesis was proposed that since the highly variable solar soft X-rays (2–10 nm) deposit their energy in the altitude region where nitric oxide has its maximum density that they are the cause of the variability of the low latitude nitric oxide [Barth *et al.*, 1988]. An analysis of the first 131 days of SNOE observations showed a correlation between the solar soft X-ray irradiance and the equatorial nitric oxide density [Barth *et al.*, 1999]. In this paper, 935 days of global observations are analyzed to determine the role that these two mechanisms play in the production of thermospheric nitric oxide.

[5] SNOE measurements of nitric oxide density in the auroral region have been compared with satellite measurements of the flux of electrons precipitating into the auroral region. The NOAA POES satellites measure the flux of

¹Laboratory for Atmospheric and Space Physics, University of Colorado, Boulder, Colorado, USA.

²Geophysical Institute, University of Alaska, Fairbanks, Alaska, USA.

³High Altitude Observatory, National Center for Atmospheric Research, Boulder, Colorado, USA.

electrons coming into the atmosphere over a large range of energies that includes the 1–10 keV interval. These measurements are reported as a hemispherical power index (HPI). The correlation of the SNOE nitric oxide densities with the NOAA HPI indicates a positive correlation [Baker *et al.*, 2001].

2. Instrument

[6] The density of nitric oxide was determined by measuring the fluorescent scattering of solar radiation at 215 and 237 nm in the (1,0) and (0,1) gamma bands using the technique of limb scanning. The instrument used was an Ebert-Fastie ultraviolet spectrometer with an off-axis telescope. The instrument parameters are given by Merkel *et al.* [2001, Table 1]. The telescope imaged the entrance slit of the spectrometer on the limb of the Earth with a field-of-view of 0.071° by 0.75° (3.1 km by 33 km) at a distance of approximately 2500 km. Photomultiplier tubes at the two exit slits measured the two ultraviolet wavelengths simultaneously. The bandpasses of both channels are 3.8 nm. The instrument was mounted on the spinning spacecraft such that the image of the slit scanned the atmosphere in the plane of the orbit forward of the spacecraft. As a result of the spinning motion of the spacecraft, the instrument also measured Rayleigh scattering from the atmosphere at 215 and 237 nm.

3. Satellite Orbit

[7] Global observations of nitric oxide in the lower thermosphere have been made from the polar orbiting SNOE spacecraft. SNOE was in a nearly circular, Sun-synchronous orbit with an inclination of 97.7° and an orbital period of 95.5 min. In March 1998, the mean altitude was 556 km with an apogee of 580 km and a perigee of 532 km. In September 2000, the mean altitude, apogee, and perigee were 526, 547, and 505 km, respectively. Nearly global coverage was achieved between 82°S and 82°N from 15 orbits per day. The spacecraft was spinning with a period of 12 sec and the spin axis was oriented perpendicular to the orbital plane. The spin period was maintained to within 1% of 12 sec throughout the mission with the use of magnetic torquing. There were 478 spins per orbit with the spacecraft moving 0.75° (91 km) along the track during the time period of one spin. The mean local time of the equatorial crossing of the orbit was 1017/2217 hours in March 1998 gradually changing to 1111/2311 hours in September 2000. The true solar local time varied throughout the year because of the varying speed of the Earth in its elliptical orbit about the Sun and because of the obliquity of the Earth's spin axis. The angle between the orbital plane of the spacecraft and the direction to the Sun (the beta angle) has been calculated for the 935 days of observations. At the equatorial crossing (the ascending node), this angle determines the true solar local time. The true solar local time and the mean solar local time are plotted in Figure 1.

[8] Limb observations were recorded when the tangential point of the view direction was between 0 and 200 km above the surface of the Earth. The integration time of each measurement was 2.4 milliseconds which corresponds to an altitude increment of approximately 3.2 km at 106 km. The

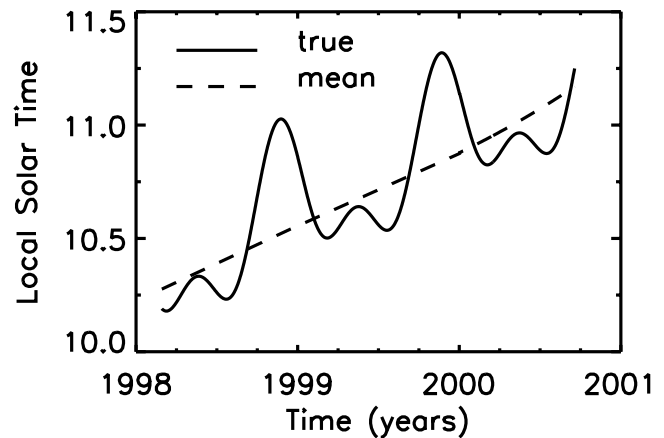


Figure 1. The true local time and the mean local time of the SNOE orbit. The mean local time on day 079 of 1998 was 1017 hours and on day 274 of 2000, it was 1111 hours.

observed point on the limb was 18° below the spacecraft orbit when viewing 200 km and 23° when viewing 0 km. The viewing direction moved downward 0.073° between successive samples. The altitude increment was nonlinear starting at 2.8 km at 200 km and increasing to 3.4 km at 0 km. For a diagram of this viewing geometry, see Merkel *et al.* [2001, Figure 2].

[9] The viewing direction of the ultraviolet telescope was determined by fitting the observed measurements of the Rayleigh scattering at 215 nm to a model of atmospheric Rayleigh scattering for the time and geometry of the observation [Merkel *et al.*, 2001]. The nonlinear altitude scale of the observations was calculated for each spin taking into account the changing altitude of the spacecraft during each orbit for the 935 days of observations. Using the technique described by Merkel *et al.* [2001], the altitude was determined with a precision of 1.5 km for each limb scan. The altitude difference between successive samples during a single spin of the spacecraft was known to better than 0.02 km. Following the altitude determination, the UVS data were interpolated onto a uniform altitude grid with altitude increments of 3.33 km between 0 and 200 km. After the calibration was applied, the result was the atmospheric radiance along the slant direction with the altitude, latitude, and longitude recorded at the tangential point. (In the SNOE UVS database, this is level one data.)

4. Calibration

[10] Both ground-based and inflight calibrations were conducted to determine the sensitivity of the ultraviolet spectrometer. In the laboratory before the flight, the sensitivity at 215 and 237 nm was determined by measuring the radiation from a deuterium lamp that was illuminating a barium sulfate scattering screen [Eparvier and Barth, 1992]. The deuterium lamp was calibrated at the Synchrotron Ultraviolet Radiation Facility of the National Institute of Standards and Technology. The reflectivity of the scattering screen was measured in the laboratory [McClintock *et al.*, 1994]. The measured sensitivity at 215 nm was 1.06 counts/kR and at 237 nm 1.11 counts/kR. The estimated uncertainty in this type of laboratory calibration is 10% [McClintock

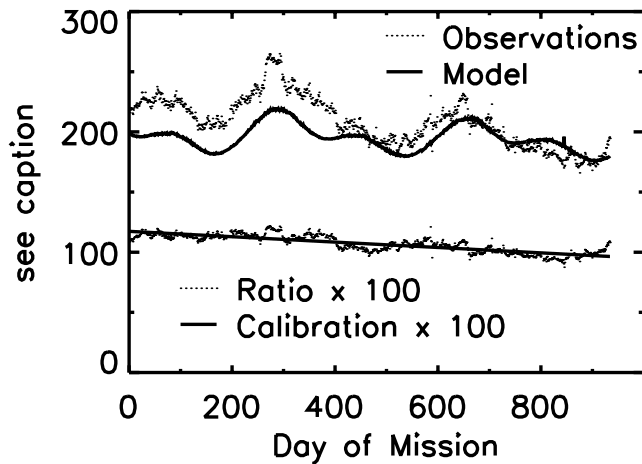


Figure 2. Time dependence of sensitivity of UVS at 237 nm. Observed atmospheric radiance at 73 km in counts per integration interval. Calculated atmospheric radiance at 73 km in kR (smoothly varying solid line). Ratio of observed radiance to calculated radiance. Time-dependent sensitivity at 237 km (straight solid line). These last two quantities have been multiplied by 100 to allow plotting on the same graph. The sensitivity of the instrument at the beginning of the mission was 1.17 counts/kR.

tock et al., 1994]. There is additional uncertainty associated with the instrument environment between calibration on the ground and operation in space.

[11] An inflight calibration was performed using the ultraviolet spectrometer measurements of the Rayleigh scattering of solar ultraviolet radiation by the atmosphere. Below about 75 km, the principal contributor to the atmospheric radiance measured by the ultraviolet spectrometer was Rayleigh scattering of solar radiation. The Rayleigh scattering contribution was measured on every spin of the spacecraft and the comparison of this observation with the calculated radiance from the atmospheric Rayleigh scattering model was used as an independent calibration of the instrument. This technique was particularly useful in determining long-term changes in the sensitivity of the photomultiplier tubes. Since the Rayleigh scattering is polarized, it was necessary to measure the polarization characteristics of the ultraviolet spectrometer in the laboratory during the calibration and to use this information in the calculation of the atmospheric Rayleigh scattering model. The daily average of the number of counts per integration interval (2.41 ms) measured in a 5° latitude band centered on the equator at an altitude of 73 km was determined. These measurements were compared to the calculated radiance from the atmospheric Rayleigh scattering model at the latitude and altitude of the observation. The results are shown in Figure 2 for 935 days of observations. The ratio of these two quantities is interpreted as the sensitivity of the instrument in counts/kR. A straight line was fit to this ratio. This result gives the sensitivity of the 237 nm channel at the beginning of this period to be 1.17 counts/kR. The sensitivity decreases at the rate of 0.0220%/day with a standard deviation of 0.0005%/day. That is a decrease in sensitivity of 20% for the 935 day period of observations. The uncertainty in the magnitude of sensitivity measured from

the Rayleigh scattering is 10% due to altitude uncertainties between the observation and the model and an additional 10% due to the uncertainties in the calibration of the polarization of the instrument. The decrease in sensitivity of the photomultiplier is most likely due to decreased electron emission from the last dynode caused by the large count rate when the instrument views the nadir.

5. Determination of Nitric Oxide Densities

[12] For both the 215 and 237 nm channels, the UVS data were sorted into 5° latitude bins centered at 0° , 5° , 10° , etc. between 82°S and 82°N geographic latitude. (Because of the inclination of the orbit, observations were not made poleward of 82° .) For each wavelength channel, the observed atmospheric radiance was compared once again with the atmospheric Rayleigh scattering model [Merkel *et al.*, 2001]. The atmospheric radiance model was normalized to the observed atmospheric radiance at 73 km. This altitude was chosen since it is above the altitude where ozone and molecular oxygen absorption occur and below the altitude where nitric oxide fluorescent scattering is significant. The observed atmospheric radiance from the 237 nm channel is plotted in Figure 3 together with the calculated Rayleigh scattering radiance. The normalized atmospheric radiance model was subtracted from the observed atmospheric radiance to remove the contribution of Rayleigh scattering. The remaining atmospheric radiance was interpreted as airglow emissions. (During the summer in the polar regions, there is some contamination below 90 km from polar mesospheric clouds.) The appropriate emission rate factor was applied to produce slant column emission rates of fluorescent scattering of nitric oxide in the (1,0) band at 215 nm and in the (0,1) band at 237 nm [Eparvier and Barth, 1992]. The (0,1) band at 237 nm is optically thin for all observed densities of nitric oxide and the (1,0) band at 215 nm may be optically thick at high nitric oxide densities. (In the SNOE UVS database, this is level two data.)

[13] For the results presented in this paper, the nitric oxide density has been determined from the 237 nm channel

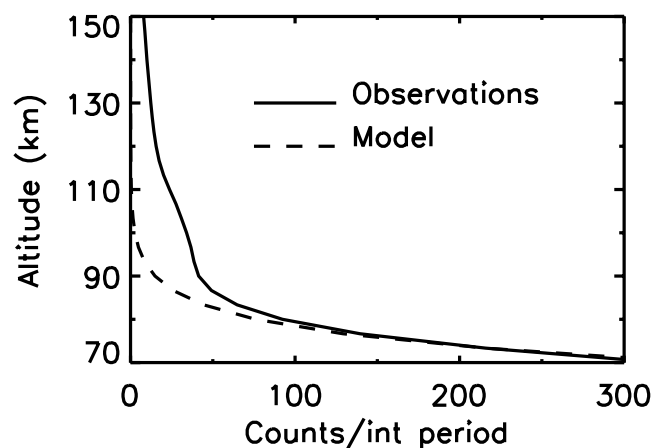


Figure 3. Comparison of atmospheric radiance observations with the calculated atmospheric Rayleigh scattering radiance model. The model is normalized to the data at 73 km. The observed radiance above 73 km is attributed to the nitric oxide airglow.

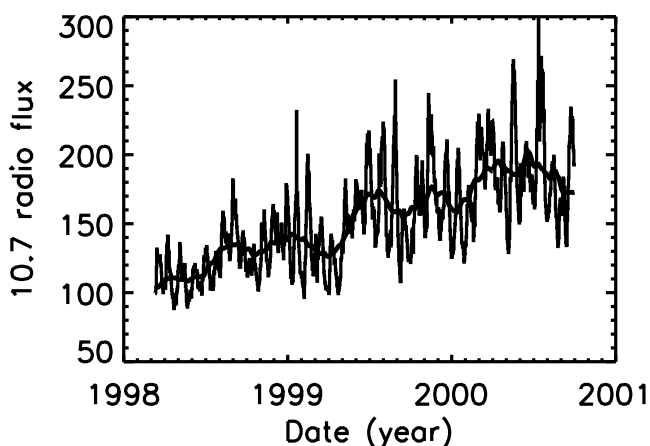


Figure 4. The 10.7 cm radio flux during the SNOE observation period.

of the UVS since the (0,1) nitric oxide gamma band is optically thin and it is not necessary to take into account self-absorption. The volume density of nitric oxide as a function of altitude has been calculated from the slant column density through the use of an onionskin inversion algorithm [McCoy, 1983]. Using this algorithm, the atmosphere was divided into 30 concentric shells, 3.3 km thick, between 70 and 170 km. The assumption was made that the volume emission rate is uniform in each shell. Taking proper account of the geometry of the path length of the instrument line of sight through each shell and of the airglow contribution above the highest shell, the volume density was determined using a matrix inversion. The emission rate factor that was used for the (0,1) band was 2.25×10^{-6} photons/sec-molecule [Eparvier and Barth, 1992]. The UVS data was processed for 15 orbits a day for 935 days as a function of altitude, geographic and geomagnetic latitude and longitude, and time. In order to minimize contamination from other airglow emissions and from polar mesospheric clouds, the altitude range was truncated to 97–150 km. Above 130 km, there still may be some contribution in the data from the molecular nitrogen Vegard-Kaplan (0–3) band [Eparvier and Barth, 1992]. (In the SNOE UVS database, this is level three data.)

[14] To produce daily averages of nitric oxide density, the fifteen orbits per day were averaged taking proper account of missing orbits and missing latitudes. (In the SNOE UVS database, this is level four data.)

6. Nitric Oxide Observations

[15] The period of nitric oxide observations between 11 March 1998 and 30 September 2000 was a time of increasing solar activity. The 10.7 cm radio flux increased from an eighty-one day mean of 100 at the beginning of the period to a mean of nearly 200 at the end (see Figure 4). Daily values ranged from about 90 up to as high as 300. On about one-third of the days the daily 10.7 cm flux was less than 132 and on one-third of the days it was above 165. During the remaining one-third of the time, the 10.7 cm flux was between these two values. There was extensive geomagnetic activity during the 935 day period. The daily A_p index is plotted in Figure 5. On one-third of the days, the daily A_p

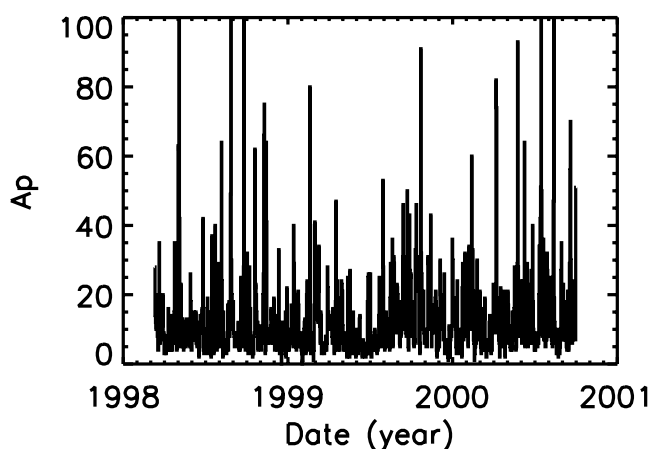


Figure 5. The geomagnetic index A_p for the SNOE observation period.

index was less than 6 and on one-third greater than 12. The remaining one-third of the days had an A_p greater than 6 and less than 12.

6.1. Altitude Profiles

[16] The solar soft X-rays have the greatest influence on the density of nitric oxide in the equatorial region. The behavior of the nitric oxide at the geographic equator was examined as a function of solar activity for the equinox periods between 20 March 1998 and 20 September 2000 (equinox plus and minus 15 days). The data set was divided into thirds using 10.7 cm radio flux values of less than 132, between 132 and 165, and greater than 165 and the mean density for these periods was calculated. Altitude profiles at low, medium, and high solar activity are plotted in Figure 6 using the 10.7 cm radio flux as an indicator of solar activity. The relationship between the solar soft X-ray flux and the 10.7 cm radio flux is described by Bailey *et al.* [2000]. The figure shows that the mean density of nitric oxide at 110 km was 8.0×10^7 molecules cm^{-3} for low activity, 1.1×10^8 molecules cm^{-3} for medium activity, and 1.3×10^8 molecules cm^{-3} for high activity. Between 97 and 123 km,

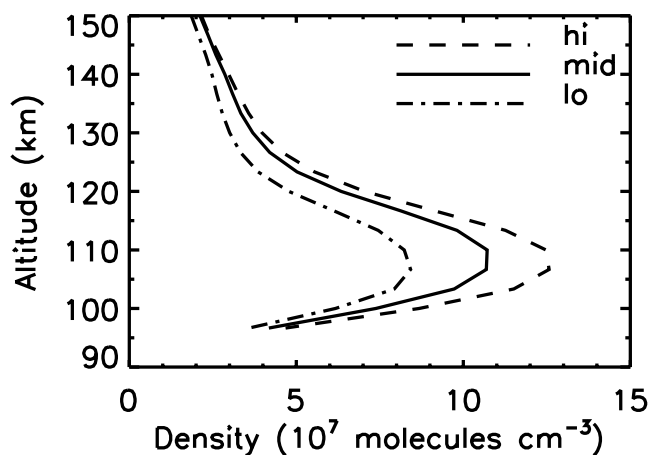


Figure 6. Altitude profiles of the mean nitric oxide density at the equator for periods of low, mid, and high solar activity.

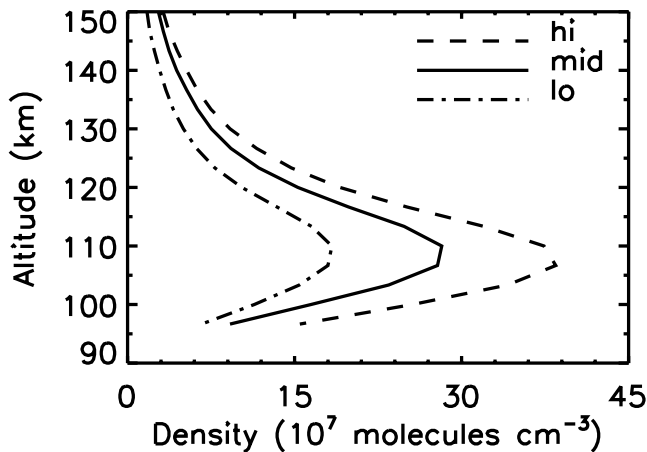


Figure 7. Altitude profiles of the mean nitric oxide density in the auroral region for periods of low, mid, and high geomagnetic activity.

the altitude profiles are proportional to each other for the three levels of solar activity indicating that this is the altitude region where the solar soft X-rays are controlling the density of nitric oxide. Above 123 km, the altitude profiles differ with different levels of solar activity.

[17] In the auroral region between 60° and 70° geomagnetic latitude, the nitric oxide density is controlled by the auroral electrons that are precipitating into the atmosphere. Nitric oxide observations in the northern auroral zone during the equinox periods (equinox plus and minus 15 days) were divided into thirds with A_p less than 6 being designated low activity, between 6 and 12 medium activity, and greater than 12 high activity. The altitude profiles of nitric oxide for these three periods are plotted in Figure 7. The mean density for low activity was 1.7×10^8 molecules cm^{-3} , for medium activity 2.7×10^8 molecules cm^{-3} , and for high activity 3.8×10^8 molecules cm^{-3} . The mean densities in the auroral zone are higher than the mean densities at the equator. The ratio of the altitude profiles are constant over the altitude range 97–123 km indicating that it is the auroral electrons that are controlling the nitric oxide densities.

6.2. Latitude–Altitude Plots

[18] Latitude–altitude plots of nitric oxide density were made for the equinox periods between 20 March 1998 and 20 September 2000 (equinox plus and minus 15 days) for one SNOE orbit. The selected orbit was chosen as the orbit where 60° – 70° geographic latitude and 60° – 70° geomagnetic latitude coincide. The choice of the equinox periods means that both auroral regions are equally illuminated by the Sun. The fluorescent scattering measuring technique requires that the nitric oxide be illuminated by solar ultraviolet radiation. Figure 8 shows the mean density of nitric oxide for 114 days during the equinox periods for all levels of solar and geomagnetic activity. This figure clearly shows the dominance of the auroral production of nitric oxide. In the auroral region, the nitric oxide density is greater than in the equatorial region and the contours of equal density extend to higher altitudes. Increased nitric oxide density extends to lower altitudes in the equatorial region. Figure 9 shows the mean nitric oxide density during the equinox

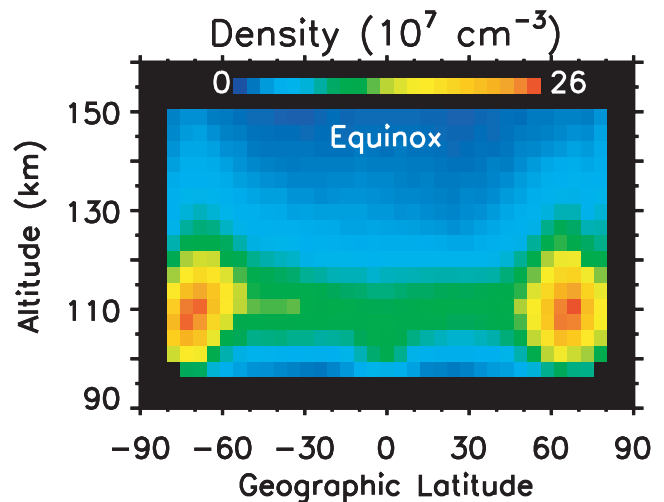


Figure 8. Latitude–altitude plot of the mean nitric oxide density for the equinox periods between day 079 of 1998 and day 274 of 2000. One orbit per day was used for 114 days of observations. The nitric oxide density in the auroral region is larger than the density in the equatorial region.

period for low levels of geomagnetic activity when the A_p index was less than 6. (There were 24 days in this sample). This figure shows that even during low geomagnetic activity, the nitric oxide density in the auroral region is larger than the density in the equatorial region. This auroral control of nitric oxide density was shown earlier from SME observations [Barth, 1992].

6.3. Time–Latitude Plots

[19] Time–latitude plots of the daily mean nitric oxide density at 106 km were made for two one-year periods starting on 20 March 1998 and 20 March 1999. In Figure 10, these plots show that the largest densities of nitric oxide occur in the auroral region near 60° – 70° latitude. The

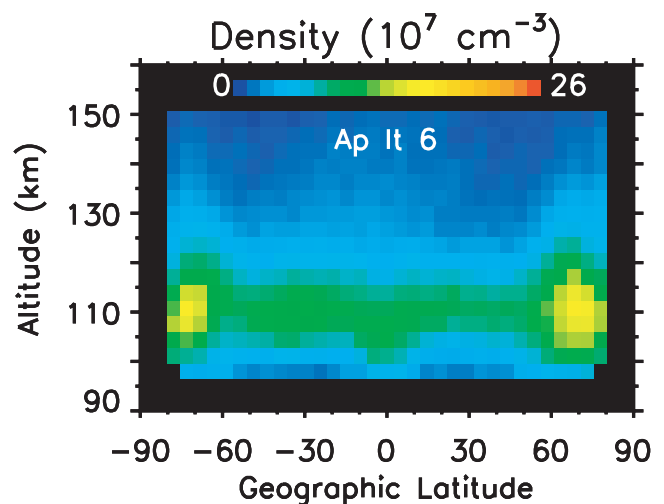


Figure 9. Latitude–altitude plot of the mean nitric oxide density for days of low geomagnetic activity ($A_p < 6$) during the SNOE equinox period. Even at low geomagnetic activity, the auroral region nitric oxide density is larger than the equatorial density.

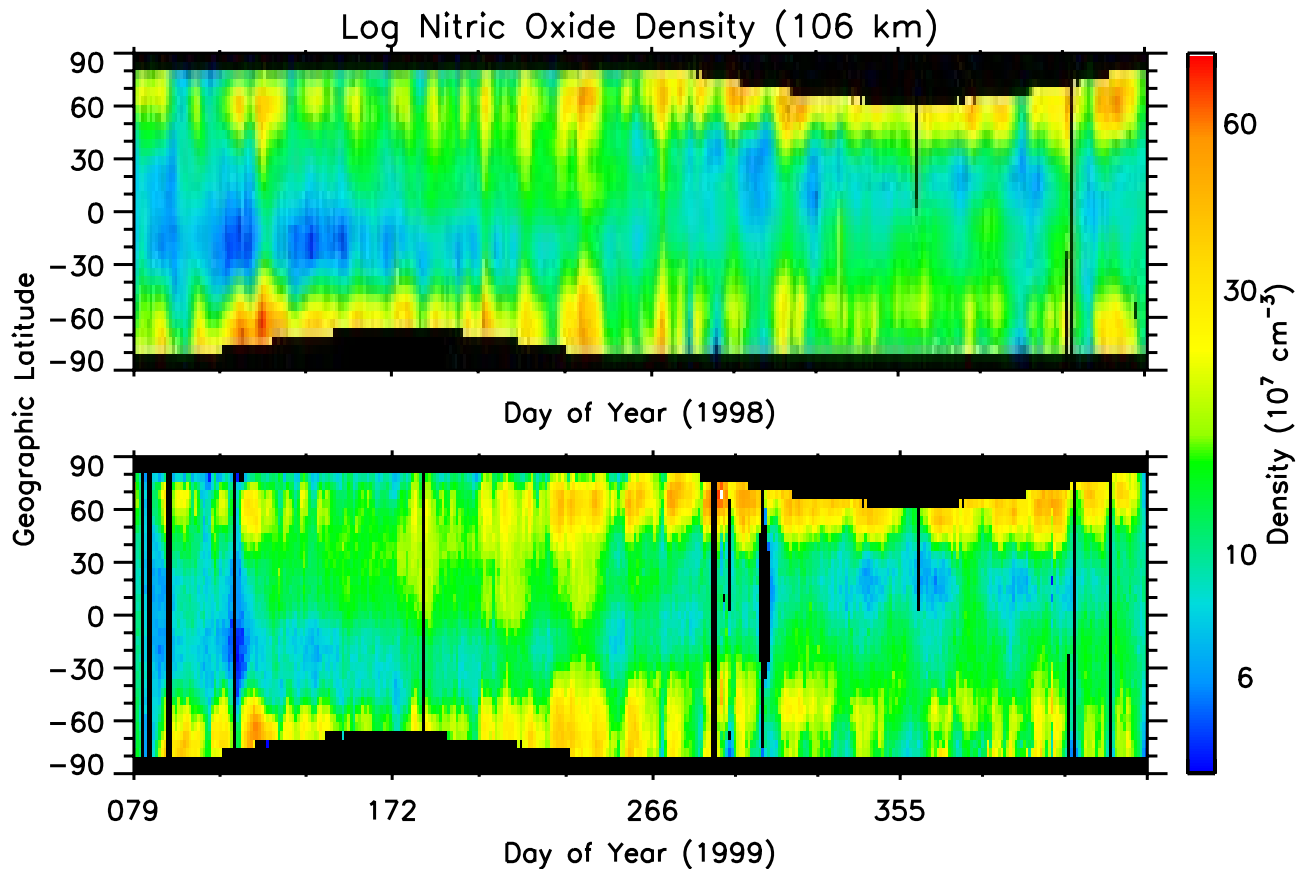


Figure 10. Time–latitude plots of daily nitric oxide densities at altitude 106 km for two one-year periods starting on day 079 of 1998 and day 079 of 1999. The largest nitric oxide densities are in the auroral region between latitudes 60° and 70°; however, there are frequent excursions of large nitric oxide densities toward the equator.

auroral nitric oxide densities vary with time since the precipitating electrons that produce the nitric oxide vary with geomagnetic activity. The nitric oxide density along the equator is less dense than at higher latitudes and also varies with time. This is the region where the solar soft X-ray flux produces the variations in the nitric oxide density. On many occasions, the large nitric oxide densities in the auroral region extend equatorward, sometimes all the way to the equator. This display of the nitric oxide density as a function of time shows seasonal effects. The black regions centered on the solstices (days 172 and 355) are periods when nitric oxide measurements were not made because the atmosphere was in darkness. The equinox periods (days 079 and 266) show both the north and south hemispheres illuminated between 82°S and 82°N. These were the periods used in the latitude–altitude plots in Figures 8 and 9. An examination of the seasonal nitric oxide densities in Figure 10 shows that the minimum densities occur south of the equator during the southern late fall and early winter. The minimum densities move north of the equator during the northern late fall and early winter. In both 1998 and 1999, the nitric oxide density in the auroral region (60°–70°) is greater in the north than in the south during the northern winter. In 1998, the auroral region nitric oxide density is greater in the south than in the north during the southern winter. Photochemical models indicate that there

should be less nitric oxide during the long periods of daylight during the summer [Bailey *et al.*, 2002]. The equinox periods appear to have large amounts of nitric oxide in the auroral regions.

[20] To examine further the equatorward motion of nitric oxide during geomagnetic storms, time–latitude plots were made of the NO density measured on individual orbits. The period chosen was the geomagnetic storm that began on day 267 of 1998, shortly after the fall equinox. A plot of the nitric oxide density at 106 km for an individual orbit during a twelve-day period that includes this geomagnetic storm is shown in Figure 11 (longitude 96°E). On the top of each nitric oxide plot, the daily average of the electron energy flux measured by the NOAA Polar Orbiting Environmental Satellites (POES) is plotted as a function of time. In this figure, the POES electron energy flux is reported as the hemispheric power which is the total electron energy flux between approximately 55°N and 75°N. The electron energy flux data shows that flux is moderate on day 267 and increases dramatically on day 268 and then decreases on the following days. In Figure 11, the nitric oxide data increases abruptly on day 269 and remains high on day 270 and then begins to decrease. This figure clearly shows the 1 day lag between the increase in electron flux and the response of nitric oxide in the region of auroral precipitation. A careful inspection of the nitric oxide density

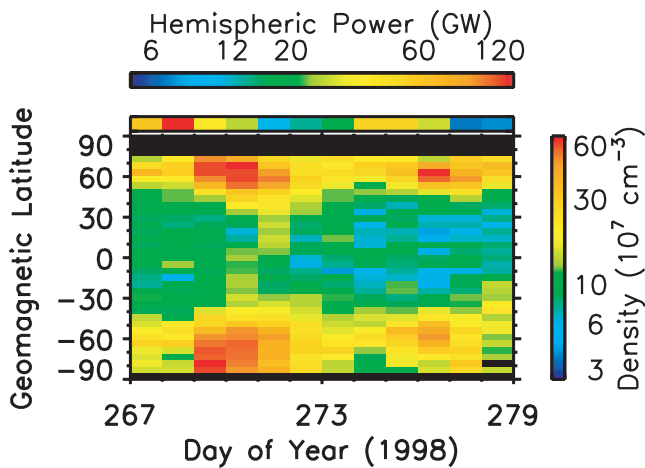


Figure 11. Time–latitude plot of nitric oxide density from a single orbit per day for a twelve-day period starting on day 267 of 1998. The bar across the top of the time–latitude plot shows the POES electron energy flux as a function of time. The POES energy flux is the total flux for the geomagnetic latitude band 55° – 75° N. The color bar above the figure applies to the POES electron energy flux. The color bar on the right side of the figure applies to the SNOE nitric oxide density. These measurements were made on a single orbit (longitude 96° E) at 0130 UT each day.

between 40° N and 75° N on days 269–271 shows apparent equatorward motion. On day 271, the increased nitric oxide extends equatorward of 30° N while the nitric oxide density at 60° N has decreased from its maximum value on day 269. This figure also shows a second geomagnetic storm starting on day 274 and lasting three days. The nitric oxide density shows the same behavior, first a lag in response to the increased electron flux and then an increase equatorward in the nitric oxide density while the density at 60° N decreases.

[21] During 935 day period from 11 March 1998 to 30 September 2000, there were approximately fifty geomagnetic storms that produced nitric oxide enhancements equatorward of the auroral zone. Many of these may be seen in Figure 10.

6.4. Interpretation

[22] The following explanation is offered for the behavior of nitric oxide in Figure 11. A large geomagnetic storm began at 2100 UT on day 267. The K_p and A_e indices increased abruptly [Baker *et al.*, 2001]. These indices remained high for 21 hours and then decreased to near normal at 1500 UT on day 268. The POES electron energy flux increased to large values on day 268. The increased electron precipitation during the storm produced increased nitric oxide in the 100–120 km region in the latitude band 55° – 75° N. Above 120 km, Joule heating in addition to direct heating from the precipitating electrons produces additional nitric oxide through a temperature-sensitive reaction of ground state atomic nitrogen with molecular oxygen [Siskind *et al.*, 1989a, 1989b]. Below 120 km, the dominant source of nitric oxide remained the reaction of excited atomic nitrogen with molecular oxygen. The most likely explanation for the presence of large amounts of nitric oxide at 106 km equatorward of the electron precip-

itation region is transport by atmospheric winds. There are no sources of production of odd nitrogen equatorward of 55° N geomagnetic latitude except for solar X-rays. An estimate of the amount of nitric oxide produced from solar X-rays may be made by looking at the nitric oxide density at the equator where no large increases are seen. In addition, the SNOE solar X-ray photometer which measured the solar X-rays [Bailey *et al.*, 2000] showed that there was not a large increase in solar X-rays during the this geomagnetic storm. The only loss process destroying the excess nitric oxide was photodissociation followed by its reaction with atomic nitrogen [Minschwaner and Siskind, 1993]. The effective lifetime of this loss process is 19.6 hours. Because of this long lifetime, nitric oxide may be used as a tracer of atmospheric motions outside of the region of electron precipitation. We believe that it was atmospheric winds with velocities of approximately 30 m/sec that carried the nitric oxide equatorward of the auroral region.

6.5. Global Observations

[23] The polar orbit of SNOE with its fifteen orbits per day provides global coverage with a longitude spacing of approximately 24° . The inclination of the orbit of 97.7° allows the observations to cover latitudes 82° S to 82° N. Global observations of the equinox periods (equinox plus and minus 15 days) are plotted in Figure 12 using orthographic projections of the northern and southern hemispheres. In this view, the geomagnetic poles (81.5° N, 82.5° W; 74.2° S, 126.1° E) are tilted toward the viewer. In each hemisphere, the maximum density of nitric oxide lies between 60° and 70° geomagnetic latitude. There is an asymmetric distribution around the auroral oval that is caused by the Earth's tilted, offset magnetic dipole field [Barth *et al.*, 2001]. In the south, the SNOE observations undersample the auroral region between 60° S and 70° S because of the large offset of the southern geomagnetic pole. In both hemispheres, the enhanced density produced by auroral electron precipitation extends equatorward to about latitude 40° .

[24] The global distribution of nitric oxide at low latitudes may be examined in Figure 13 that uses a cylindrical projection of nitric oxide densities. The minimum density lies between 10° S and 10° N geomagnetic latitude following the geomagnetic equator. For this data set, the minimum density is off the coast of South America at 15° S, 108° W. This figure also shows the undersampling of the southern auroral region between 150° W and 30° E.

7. Correlations

[25] The question of how far equatorward does the influence of electron precipitation extend was addressed by performing correlations between various geomagnetic latitude bands in the northern hemisphere. The data set consists of 935 days of observations in fourteen latitude bands. The latitude band at 65° N was chosen as an indicator of the flux of precipitating auroral electrons (auroral source). The latitude band at 0° was used as a measure of the flux of solar soft X-rays (solar X-ray source). The twelve 5° latitude bands lying between these two were studied in a multiple regression analysis. The

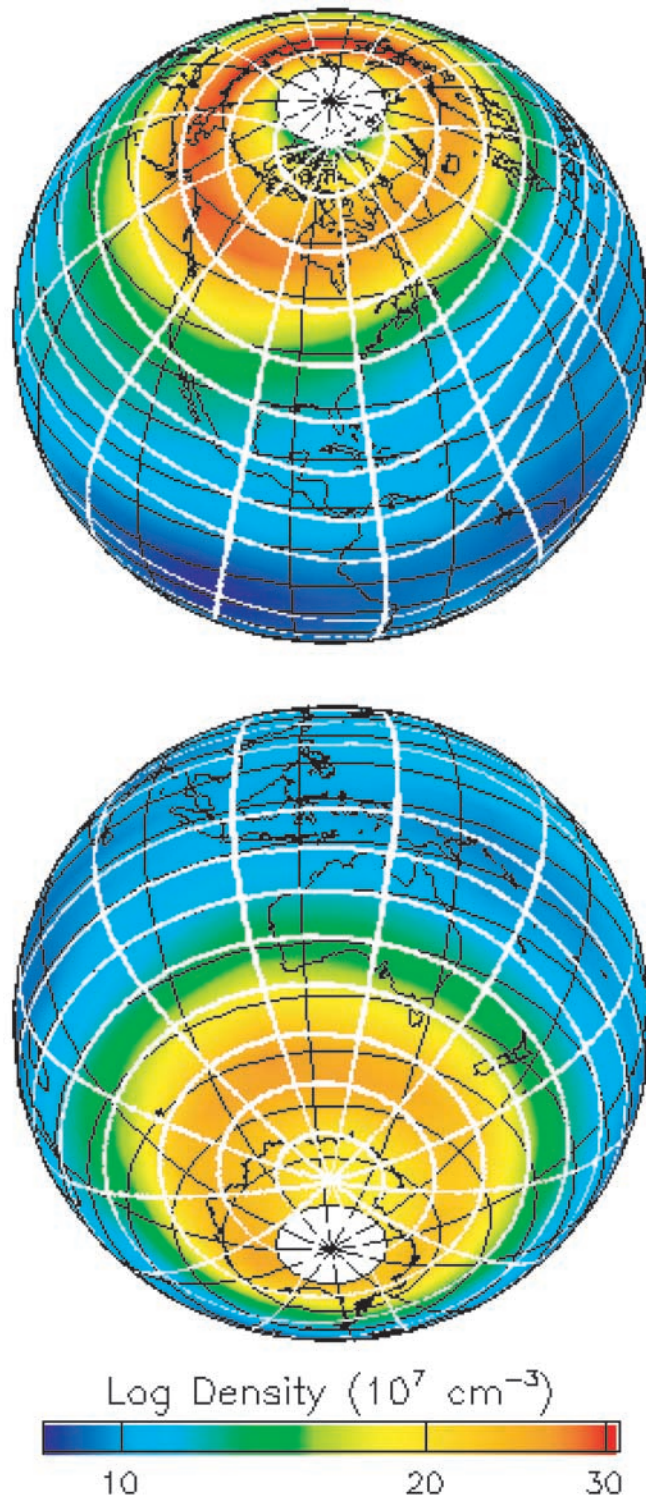


Figure 12. Global images of the mean nitric oxide density for the SNOE equinox periods. Geomagnetic latitude and longitude are plotted as white lines. The largest amount of nitric oxide occurs in the auroral region between 60° and 70° geomagnetic latitude. In each hemisphere, the geomagnetic poles are tilted toward the viewer.

nitric oxide density at the equator for the 935 day period is plotted in Figure 14. The nitric oxide density in the auroral region is plotted in Figure 15. These two data sets are not correlated. The equatorial densities are controlled by solar

activity (solar soft X-rays) and the auroral densities are the result of magnetospheric activity (1–10 keV precipitating electrons). A multiple regression was performed on each of the twelve bands to determine the influence of the

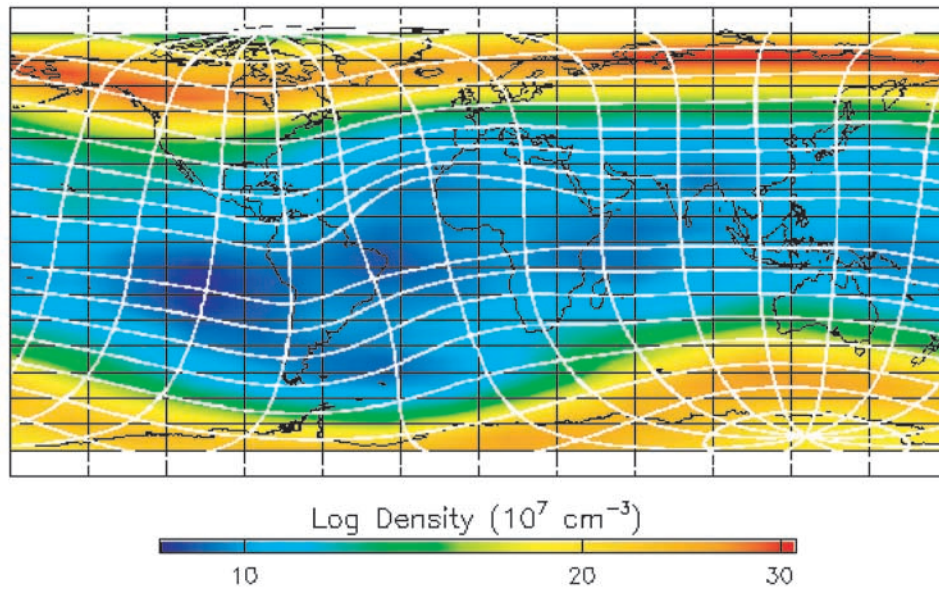


Figure 13. Global plot of the mean nitric oxide density for the SNOE equinox periods in cylindrical coordinates. Geographic latitude and longitude are plotted as black lines. Geomagnetic latitude and longitude are plotted as white lines. The minimum density of nitric oxide follows the geomagnetic equator.

equatorial and auroral sources of nitric oxide on the density at each geomagnetic latitude. The results are presented in Table 1.

[26] The first column in the table lists the latitude band and the last column shows the multiple regression coefficients. Near the equator and near the auroral region, the correlation coefficient is high. Columns two and three give the percent contribution of the equatorial and the auroral sources to the nitric oxide density at each latitude. For latitudes 0° – 30° , the solar soft X-ray source contributes over 95% to the variability of nitric oxide. For latitude 60° N, the auroral source (1–10 keV electrons) contributes 89% and the equatorial source 11%. A significant result from this analysis is that at midlatitudes, 40° – 50° N, there is a significant contribution from the auroral electron source throughout the 935 day period.

[27] The solar soft X-ray irradiance has been measured from the SNOE spacecraft during the 935 days of this analysis [Bailey *et al.*, 2000]. Calculations with a photochemical model have shown that solar X-rays in the 2–7 nm wavelength range should have the greatest effect on the production of nitric oxide in the altitude range 100–120 km [Bailey *et al.*, 2002]. To test this idea, a series of correlations were calculated using the SNOE solar X-ray 2–7 nm and equatorial nitric oxide data. Initially, the altitude of 106 km and a latitude band between 5° S and 5° N was chosen for the nitric oxide data. (See Figure 6 for the altitude profile.) It was found that the correlation between the X-ray data and the nitric oxide data was better when the solar X-ray data from the previous day was used. A linear fit was made to these data sets taking into account that both data sets vary independently. The results are plotted in Figure 16. The correlation

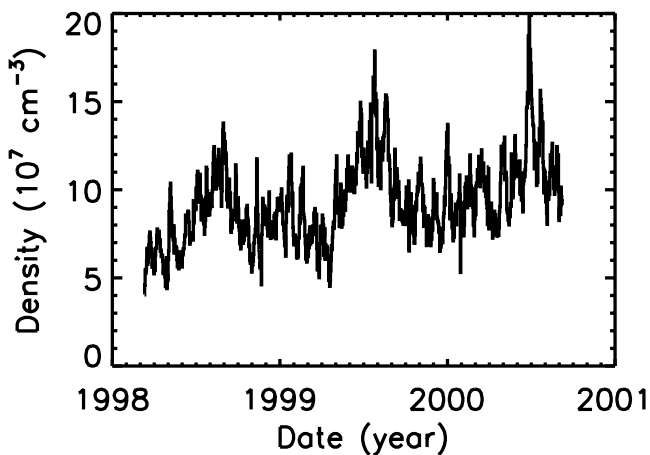


Figure 14. Equatorial nitric oxide density at 106 km for 935 days.

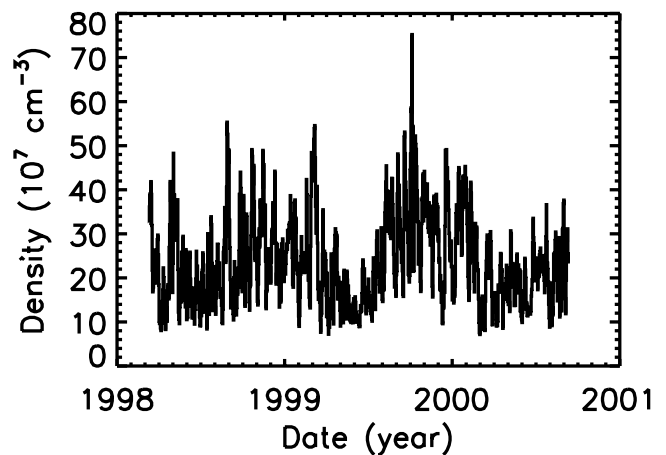


Figure 15. Auroral nitric oxide density (65° N) at 106 km for 935 days.

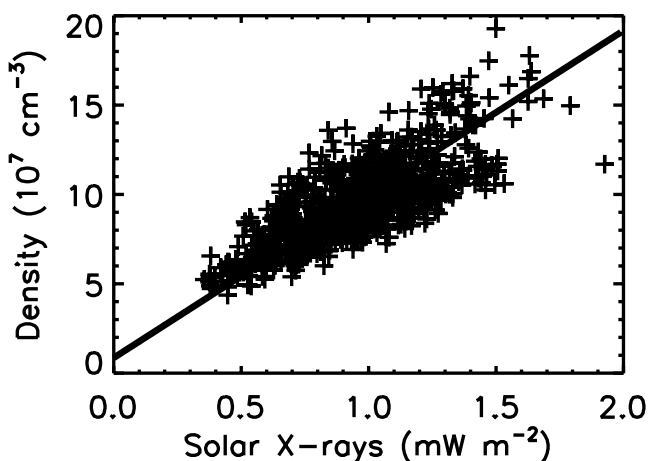
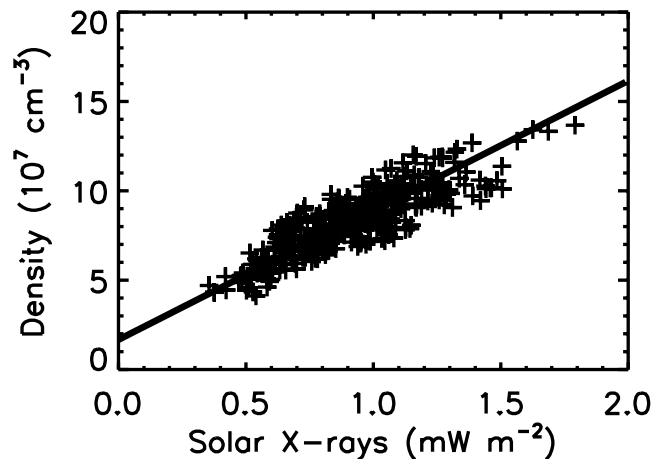
Table 1. Contribution of Equatorial and Auroral Sources of Nitric Oxide as a Function of Latitude

| Geomagnetic Latitude, °N | Solar X-Ray Source, % | Auroral Source, % | Multiple Regression Coefficient |
|--------------------------|-----------------------|-------------------|---------------------------------|
| 0 | 100 | 0 | 1.00 |
| 5 | 100 | 0 | 0.95 |
| 10 | 100 | 0 | 0.92 |
| 15 | 100 | 0 | 0.88 |
| 20 | 100 | 0 | 0.86 |
| 25 | 98 | 2 | 0.83 |
| 30 | 95 | 5 | 0.80 |
| 35 | 87 | 13 | 0.76 |
| 40 | 75 | 25 | 0.72 |
| 45 | 62 | 38 | 0.73 |
| 50 | 45 | 55 | 0.78 |
| 55 | 28 | 72 | 0.86 |
| 60 | 11 | 89 | 0.95 |
| 65 | 0 | 100 | 1.00 |

coefficient for this calculation is 0.76, the slope of the line is 9.2 and the intercept is 0.86. Additional comparisons between these two data sets were made. The altitude of the nitric oxide data was varied and it was found that a better correlation occurred at 113 km. The data sets were then restricted to those days when auroral electron precipitation in the auroral region was low. This was done by using the observed nitric oxide density at 65°N to establish the criteria. The selected data sets contained 384 days. The linear fit that was made to the solar X-ray and equatorial nitric oxide data is shown in Figure 17. The correlation coefficient is 0.86, the slope 7.2 and the intercept is 1.7. The variation of correlation coefficients with the altitude of the nitric oxide is given in Table 2. This table shows the altitude region where solar X-rays play a significant role in the production of nitric oxide in the equatorial region.

8. Discussion

[28] All of the observations of nitric oxide that have been presented in this paper are consistent with the paradigm of two sources of production of nitric oxide in the thermosphere [Barth, 1992]. The first source is the solar soft X-ray

**Figure 16.** Correlation of equatorial nitric oxide (106 km) with solar X-rays (2–7 nm) for 935 days of observations. The correlation coefficient is 0.76, the slope is 9.2, and the intercept is 0.86.**Figure 17.** Correlation of equatorial nitric oxide (113 km) with solar X-rays (2–7 nm). To minimize the contribution of nitric oxide produced by auroral electron precipitation, the data set was restricted to days with low auroral activity (384 days). The correlation coefficient is 0.86, the slope is 7.2, and the intercept is 1.7.

irradiance in the 2–7 nm wavelength region which is effective over the entire illuminated hemisphere but with its maximum effect in the equatorial region at the subsolar point. The best evidence for the solar X-ray mechanism is the correlation between solar X-rays and nitric oxide density shown in Figure 17. When the influence of the auroral electron precipitation mechanism is minimized, the correlation coefficient of 0.86 is indicative of a good correlation. The remaining lack of correlation is probably because each of the data sets are one day averages in time. The finite intercept of $1.7 \times 10^7 \text{ cm}^{-3}$ may mean that there is an additional nonvarying source of nitric oxide. The fact that the correlation of the X-rays with nitric oxide is better at 113 km than at the density maximum at 106 km means that vertical mixing is carrying nitric oxide downward since the mixing ratio of nitric oxide at 113 km is larger than at 106 km. The idea that solar soft X-rays were the source of low latitude nitric oxide was first offered as a hypothesis [Barth *et al.*, 1988] and then calculations showed a possible effect on thermospheric nitric oxide [Siskind *et al.*, 1990]. It has been the simultaneous measurements of solar soft X-rays and thermospheric nitric oxide from SNOE that have

Table 2. Correlation of Solar X-Rays With Nitric Oxide as a Function of Altitude

| Altitude, km | Correlation Coefficient | Density, 10^7 cm^{-3} |
|--------------|-------------------------|---------------------------------|
| 140.0 | 0.46 | 2.5 |
| 136.7 | 0.51 | 2.7 |
| 133.3 | 0.55 | 2.9 |
| 130.0 | 0.66 | 3.2 |
| 126.7 | 0.69 | 3.5 |
| 123.3 | 0.74 | 4.2 |
| 120.0 | 0.79 | 5.2 |
| 116.7 | 0.83 | 6.7 |
| 113.3 | 0.86 | 8.2 |
| 110.0 | 0.81 | 9.2 |
| 106.7 | 0.75 | 9.3 |
| 103.3 | 0.71 | 8.6 |
| 100.0 | 0.62 | 6.5 |

confirmed that this is the dominant low-latitude mechanism, first with 131 days of observations [Barth *et al.*, 1999] and now with 935 days of simultaneous measurements. The two and a half years of SNOE observations cover a complete range of seasons during a period of solar activity that was increasing from near minimum to near maximum.

[29] The second source of nitric oxide is the auroral electron precipitation (1–10 keV) at high geomagnetic latitudes. SNOE observations of nitric oxide in the auroral region (60°–70° geomagnetic latitude) show how the nitric oxide varies with geomagnetic activity. There are seasonal effects as well. In addition, the SNOE global measurements of nitric oxide show that there is nitric oxide at midlatitudes equatorward of the auroral region that has its source in the auroral region. This is shown by the correlations of the variations of the midlatitude nitric oxide density with the variations of the auroral region nitric oxide density using the 935 days of observations. There is increased nitric oxide above 120 km during geomagnetic storms as a result of Joule heating [Siskind *et al.*, 1989a, 1989b]. Heat may be transported equatorward enhancing the production of nitric oxide above 120 km at midlatitudes. However, the largest density of nitric oxide which occurs at 106–110 km is produced by 1–10 keV electrons precipitating into the auroral region (60°–70° geomagnetic latitude). The presence of nitric oxide at 106 km at midlatitudes may be the result of atmospheric winds. The time–latitude plots show what appears to be equatorial movement of nitric oxide toward the equator.

[30] This two and a half year data set of global observations of nitric oxide may be used as a test for three-dimensional models of the thermosphere. The precipitating auroral electrons that produce nitric oxide also heat the thermosphere. The heating leads to atmospheric motions that affect the distribution of nitric oxide. The SNOE data set shows the global distribution of nitric oxide every day for 935 days. Geomagnetic storms dramatically changed the nitric oxide density distribution during this period. The successful modeling of the nitric oxide distribution during a geomagnetic storm would increase the credibility of a three-dimensional model's ability to calculate ionization, heating, and atmospheric motions.

9. Summary

[31] Global observations of thermospheric nitric oxide have been obtained for the two and a half year period 11 March 1998 to 30 September 2000. These observations confirm that there are two major sources of nitric oxide in the thermosphere. One is the result of the action of solar soft X-rays (2–7 nm) on the major constituents. The solar soft X-ray source dominates in the equatorial region, but affects the density of nitric oxide over the entire illuminated hemisphere. The second source is the result of the action of auroral electrons (1–10 keV) precipitating into the thermosphere from the magnetosphere. This source dominates in the auroral region (60°–70° geomagnetic latitude), but its influence extends to midlatitudes as well. During geomagnetic storms, nitric oxide is present at midlatitudes equatorward of the auroral region. The presence of nitric

oxide at midlatitudes may be the result of meridional winds that carry the nitric oxide equatorward.

[32] **Acknowledgments.** The Student Nitric Oxide Explorer (SNOE) mission was managed for the National Aeronautics and Space Administration by the Universities Space Research Association. The preparation of the SNOE data for the National Space Science Data Center (NSSDC) was sponsored by a grant from NASA Headquarters. We appreciate the help of David Evans of the National Oceanic and Atmospheric Administration in interpreting the Polar Orbiting Environmental Satellite data [www.sec.noaa.gov].

References

- Bailey, S. M., T. N. Woods, C. A. Barth, S. C. Solomon, L. R. Canfield, and R. Korde, Measurements of the solar soft x-ray irradiance by the Student Nitric Oxide Explorer: First analysis and underflight calibrations, *J. Geophys. Res.*, *105*, 27,179–27,193, 2000.
- Bailey, S. M., C. A. Barth, and S. C. Solomon, A model of nitric oxide in the lower thermosphere, *J. Geophys. Res.*, *107*(A8), 1206, doi:10.1029/2001JA000258, 2002.
- Baker, D. N., C. A. Barth, K. D. Mankoff, S. G. Kanekal, S. M. Bailey, G. M. Mason, and J. E. Mazur, Relationships between precipitating auroral zone electrons and lower thermospheric nitric oxide densities: 1998–2000, *J. Geophys. Res.*, *106*, 24,465–24,480, 2001.
- Barth, C. A., Nitric oxide in the lower thermosphere, *Planet. Space Sci.*, *40*, 315–336, 1992.
- Barth, C. A., D. W. Rusch, and A. I. Stewart, The UV nitric-oxide experiment for Atmosphere Explorer, *Radio Sci.*, *8*, 379–385, 1973.
- Barth, C. A., W. K. Tobiska, D. E. Siskind, and D. D. Cleary, Solar–terrestrial coupling: Low-latitude thermospheric nitric oxide, *Geophys. Res. Lett.*, *15*, 92, 1988.
- Barth, C. A., S. C. Bailey, and S. C. Solomon, Solar–terrestrial coupling: Solar soft x-rays and thermospheric nitric oxide, *Geophys. Res. Lett.*, *26*, 1251–1254, 1999.
- Barth, C. A., D. N. Baker, K. D. Mankoff, and S. M. Bailey, The northern auroral region as observed in nitric oxide, *Geophys. Res. Lett.*, *28*, 1463–1466, 2001.
- Eparvier, F. G., and C. A. Barth, Self-absorption theory applied to rocket measurements of the nitric oxide (1,0) γ band in the daytime thermosphere, *J. Geophys. Res.*, *97*, 13,723–13,731, 1992.
- Gerard, J. C., and C. A. Barth, High-latitude nitric oxide in the lower thermosphere, *J. Geophys. Res.*, *82*, 674–680, 1977.
- McClintock, W. E., C. A. Barth, and R. A. Kohnert, Sulfur dioxide in the atmosphere of Venus, 1, Sounding rocket observations, *Icarus*, *112*, 382–388, 1994.
- McCoy, R. P., Thermospheric odd nitrogen, 1, NO, N(4S), O(3P) densities from rocket measurements of the NO delta and gamma bands and the O₂ Herzberg I bands, *J. Geophys. Res.*, *88*, 3197–3205, 1983.
- Merkel, A. W., C. A. Barth, and S. M. Bailey, Altitude determination of ultraviolet measurements made by the Student Nitric Oxide Explorer, *J. Geophys. Res.*, *106*, 30,283–30,290, 2001.
- Minschwaner, K., and D. E. Siskind, A new calculation of nitric oxide photolysis in the stratosphere, mesosphere, and lower thermosphere, *J. Geophys. Res.*, *98*, 20,401–20,412, 1993.
- Rusch, D. W., and C. A. Barth, Satellite measurements of nitric oxide in the polar region, *J. Geophys. Res.*, *80*, 3719–3721, 1975.
- Siskind, D. E., C. A. Barth, and R. G. Roble, The response of thermospheric nitric oxide to an auroral storm, 1, Low and middle latitudes, *J. Geophys. Res.*, *94*, 16,885–16,898, 1989a.
- Siskind, D. E., C. A. Barth, and R. G. Roble, The response of thermospheric nitric oxide to an auroral storm, 2, Auroral latitudes, *J. Geophys. Res.*, *94*, 16,899–16,911, 1989b.
- Siskind, D. E., C. A. Barth, and D. D. Cleary, The possible effect of solar X-rays on thermospheric nitric oxide, *J. Geophys. Res.*, *95*, 4311–4317, 1990.

S. M. Bailey, Geophysical Institute, University of Alaska, Fairbanks, AK 99775-7320, USA. (scott.bailey@gi.alaska.edu)

C. A. Barth and K. D. Mankoff, Laboratory for Atmospheric and Space Physics, University of Colorado, Boulder, CO 80309-0590, USA. (charles.barth@lasp.colorado.edu)

S. C. Solomon, High Altitude Observatory, National Center for Atmospheric Research, Boulder, CO 80307, USA. (stans@hao.ucar.edu)